Proceedings of the Estonian Academy of Sciences,
2020, **69**, 3, 257–265
https://doi.org/10.3176/proc.2020.3.08
Available online at www.eap.ee/proceedings

LASER CLADDING

Study of the impact of the powder laser cladding position on the parameters of the cladded layer

Andris Ratkus* and Toms Torims

Department of Mechanical Engineering and Mechatronics, Faculty of Mechanical Engineering, Transport and Aeronautics, Riga Technical University, Kipsala Str. 6B, Riga, LV-1048, Latvia

Received 17 January 2020, accepted 8 June 2020, available online 16 July 2020

Abstract. This research describes the realization of a hitherto unexplored aspect of laser cladding technology – laser cladding with powder – to provide cladding in the overhead (OH) position. This position is important for bore claddings where objects are large and the bore cannot be orientated vertically to ensure a constantly vertical cladding position, or when the object cannot be secured in a chuck and rotated to provide a constantly flat (F) cladding position. Laser cladding experiments have been performed to determine the dependence of the laser cladding characteristics on the cladding position and nozzle angle. Safe laser cladding using powder and a coaxial nozzle in the OH position is possible with a nozzle angle $\alpha = 36°$. In the paper, mathematical expressions were developed for predicting such characteristics as the cladding thickness (H), cladding area (A_C) and dilution (D_C) of the laser cladding technology, by introducing the parameter G, in which the obtained results are predictable and useful. The introduced parameter G consists of the above laser cladding parameters combined with simple equations, making it possible to predict the results. It has been experimentally proved that laser cladding with powder can be successfully implemented in the flat (F), vertical up (VU), overhead (OH) and vertical down (VD) positions, therefore laser cladding with powder can be used for bore claddings. The influence of the positions F, VU, OH and VD on the cladding characteristics H, A_C and D_C has been experimentally determined. Hardness measurement results show a correlation between the melt pool temperature distribution and microhardness (HV) values. The knowledge acquired in this research is adaptable and also applicable to the development of external surface cladding.

Key words: powder laser cladding, predicting cladding characteristics, Stellite® 6.

1. INTRODUCTION

There is growing industrial demand for surface renewal and modification technologies such as laser cladding, which restore and improve the performance characteristics of the base material[1]. The versatility of laser cladding technology has led to its fast-growing usage in an increasing number of applications due to the following features: the technology is suitable for a wide range of materials; it has a high and easily controlled energy density, a short processing time, a small heat-affected area and an excellent degree of cladding dilution [1].

These benefits of the laser cladding technology, along with its accessibility, have encouraged researchers to seek out new laser cladding applications. Therefore, the authors of this research are looking for possibilities to use laser cladding technology with powder in renewal applications, specifically in bore cladding technologies, given their experience in this field. Laser cladding technology with powder (hereinafter 'laser cladding') is also a very widespread technology, thus offering a broad range and accessibility of materials [2].

Bores that potentially require restoration form part of large, expensive equipment items that are found in

* Corresponding author, andris.ratkus@gmail.com
[1] The number of research articles with keywords "laser cladding" at www.sciencedirect.com has been growing constantly since the year 2013.

excavator frames and mining equipment housing, etc., where renewal technologies are preferred owing to the relatively low cost of repair compared to replacing the entire damaged unit. Typically, these frames and housings are made from S355J2 type construction steel. For bore renewal operations, the most important process is the cladding of the new material layer and in this research, the authors will focus only on this process. Laser cladding technology know-how does not basically differ, whether it is used for repair or material surface modification operations. Therefore, the term 'laser cladding' will be used to refer to the new material layer creation operation.

In industry, several types of equipment have been identified as being suitable for internal bore laser cladding, e.g., an apparatus patented by the Fraunhofer USA [3] and ID 2 – Internal Cladding Head, Fraunhofer USA CLA. The Fraunhofer Institute for Material and Beam Technology IWS has also produced the inner diameter coating system COAXid [4], describing it as a "*Direction-independent powder feed for complex inner surfaces*", i.e. a cladding nozzle that can produce cladding in any direction when the nozzle moves over a certain horizontal or vertical plane, but the nozzle cannot work in the overhead (OH) position. Cladding with these nozzles can be performed in cylindrical shells and pipes which can be fastened and rotated in the chuck to provide a single, flat (F) or vertical (V) laser cladding position. Here the nozzle is moving only in an axial direction in the bore, whilst the other movements are achieved by the chuck on which the cladded object is mounted.

Another alternative for the bore laser cladding application is equipment for medium sized objects such as transmission housings and engine blocks, where the whole object cannot be fixed and rotated in a chuck, but it is possible to orientate the bore vertically. This type of equipment has also been developed [5], where the vertically orientated bore provides a stationary V laser cladding position.

But for large pieces of industrial equipment, it is nearly impossible to place them on stationary workshop machines due to the size and irregular configuration, or to orient it to provide a constant laser cladding position. There are also inevitable situations where the borehole is located horizontally, making it necessary to clad in the OH position. This means that all the aforementioned nozzles [3–5] cannot be used, because the result cannot be guaranteed in the OH position. Moreover, no other studies regarding OH laser cladding are known to the authors. Therefore, this research is focusing on bore cladding results for OH and other cladding positions on a macro scale.

Examination of state-of-the-art laser cladding research reveals plenty of successful researches [6–10] in terms of laser cladding parameters and results. Also, the experimental aspects are sufficiently described, so that these studies can be used as examples in the selection of parameters.

The main objective and novelty of this research is to identify the potential of laser cladding technology for cladding in various positions, especially the OH position, to identify the influence of technological parameters on the results, and to draw up mathematical expressions for predicting single (not area cladding) laser cladding results.

2. LASER CLADDING EXPERIMENT

This chapter identifies the technological parameters and characteristics of the laser cladding, as applied and controlled in the experimental work. The characteristics and parameters were chosen to validate the application of the laser cladding technology and also to enable a mutual mathematical comparison with other authors' researches.

In this chapter we describe the choice of the most important laser cladding equipment, the nozzle, as well as listing the other equipment items and materials used.

2.1. Laser cladding technological and process parameters

The following technological parameters were varied and monitored in the laser cladding experiment: the cladding speed (v, m/min), the laser power (P, W), the powder feed (F_{pm}, g/min) and the track distance (f, mm/rev.).

The range of technological parameters that were used in the reviewed literature and which offered good results, are summarized in Table 1 [6–10].

The parameters of the cladding process were measured during the experimental work: recording the temperature of the melt pool by means of the "*E-MAqS*"[2] (Fraunhofer IWS) system. The system records the image element during the laser cladding process – the number of pixels (T_A) at which the temperature is the same or higher than the set temperature.

Melting efficiency (E_{pm}, %) is used to describe the percentage of the delivered material that is cladded to the base material.

Table 1. Range of suitable laser cladding technological parameters for laser beam with spot size of 4 mm

P, W	v, m/min	F_{pm}, g/min
1100–2000	0.5–0.8	10–33

[2] https://www.iws.fraunhofer.de/en/business_fields/surface_treatment/surface_treatment/products/e-maqs.html

Laser intensity (I_{LP}, W/mm^2) describes the power density on the base material, while the powder feed intensity (I_{PF}, %) is used to describe the amount of powder that is delivered into the laser spot.

2.2. Laser cladding characteristic parameters

The following cladding characteristic parameters were determined in the experiment:

1. Cladding thickness h (Fig. 1).
2. Cladding area A_c (Fig. 1).
3. Melt pool depth p (Fig. 1).
4. The cladding dilution D_c determined by expression (1) given the melting area A_b and A_c (Fig. 1) [11].

$$D_c = \frac{A_b}{A_b + A_c}. \quad (1)$$

5. The microhardness of the cross-section of the cladding (HV), which describes the material mechanical properties of the cladded and base layers. These microhardness measurements are made to identify and compare the mechanical properties of the new layer of the material and base material.

2.3. Nozzle used for the laser cladding experiment

Analysis of the laser cladding literature identified various laser cladding nozzles, which differ mainly according to the type of material supplied and the method of material input [1]. As mentioned before, powder will be used as the cladding material. It is also known that the bore cladding equipment [3–5] is subject to several restrictions, to ensure the result at the required OH position complies with safety standards. The nozzles are compact, using laser optics close to the cladding area and the nozzle angle is perpendicular ($\alpha = 90°$). From the authors' experience with COAXid [4], even at F position there is a risk of the optics being damaged by the reflecting laser beam and powder. Therefore, the universal cladding nozzle COAX12, developed by the Fraunhofer IWS Institute, was used. For COAX12, the distance between the cladding area and the optical elements is approximately 200 mm (depending on the setup). The nozzle is suitable for cladding complicated configurations, involving a range of travel directions at the nozzle angle (α), because the powder is delivered from 4 powder bores located around the laser spot [12].

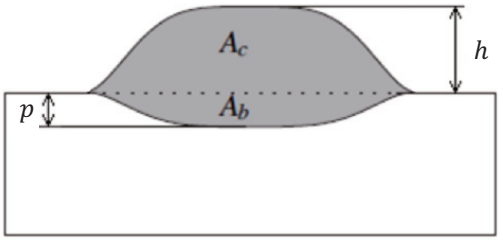

Fig. 1. Cross-section of the cladding [11].

To avoid the risk of damaging the COAX12 nozzle in the OH position, the cladding was achieved by using the nozzle angle $\alpha = 36°$. Cladding in positions F, vertical up (VU) and vertical down (VD) at a nozzle angle $\alpha = 36°$ was undertaken to ensure not only the comparability of results, but also to simulate bore cladding conditions. The laser cladding experiment was conducted on flat surfaces located in the scheme positions F, VU, OH and VD (Fig. 2).

The influence of the nozzle angle variations ($\alpha = 90°$; 81°; 63°; 45°; 36° in the cladding position F) on cladding characteristics was tested in experimental work and extended the amount of information obtained.

2.4. Equipment and materials used in the experiment

The laser cladding experiment was performed using the following equipment:

1. Nozzle COAX12.
2. Diode laser source – LDF diode laser LDF 20000–200, Laserline GmbH.
3. Manipulator – industrial robot KR 60HA, KUKA Roboter GmbH.
4. Powder feeder – GTV-Powder feeder MF-PF 2/2, GTV Verschleißschutz GmbH.

The following materials were used in the laser cladding experiment:

1. Steel flat bar S355J2 (EN 10025-2) [13] (350 mm × 80 mm × 12 mm), surface roughness Rz 25 μm.
2. Powder: Stellite® 6, nominal powder particle size 150 μm/63 μm (Table 2).
3. Powder transport gas (Ar) 3 l/min; protective gas (Ar) 15 l/min.

Before cladding, grease, lubricants and dust were removed from the surface of the base material using alcohol.

Stellite® 6 powder is widely used in industry because it provides very good mechanical properties: high wear resistance, corrosion resistance even at high temperatures (500 °C), and expected microhardness HV 450–550 kg/mm^2 [7].

2.5. Technological parameters of the experiment

Considering the information summarized in Table 1 and the authors' practical knowledge, Table 3 lists the technological parameters of the laser cladding research.

2.6. Laser cladding and hardness of the base material

Cladding microhardness measurements were taken to verify the mechanical properties of cladding and base

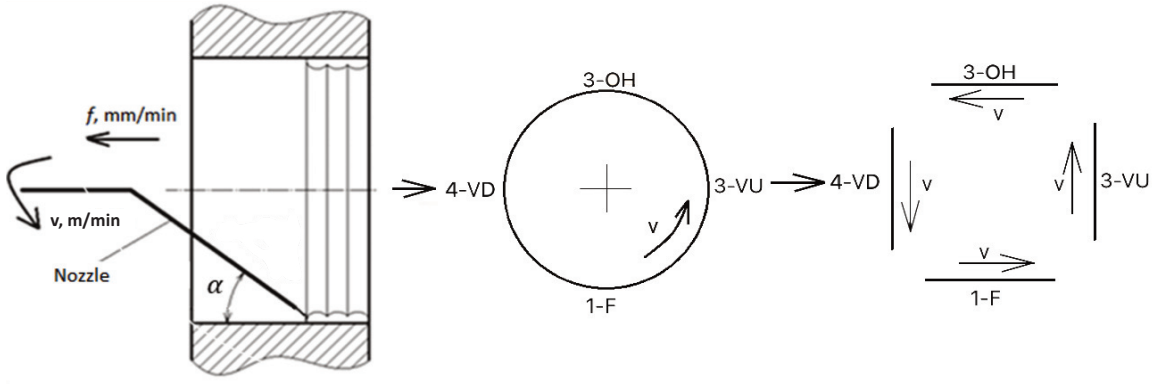

Fig. 2. Laser cladding experiment scheme.

Table 2. Nominal chemical composition of the cladding powder Stellite® 6 [14]

Co, %	Cr, %	W, %	C, %	Other
Base	27–32	4–6	0.9–1.4	Ni, Fe, Si, Mn, Mo

Table 3. Technological parameters of the laser cladding experiment

Sample	1	2	3	4	5	6	7	8
P, kW	1.66	1.66	1.66	2.04	2.04	2.04	1.2	1.4
v, m/min	0.5	0.65	0.8	0.5	0.65	0.8	0.5	0.5
F_{pm}, g/min	30.7	30.7	30.7	32.9	32.9	32.9	14	25

material. Measurements of microhardness (HV) according to the Vickers hardness test (EN ISO 6507–1:2018) were performed during the work (weight 1.98 N, measuring time 10 s).

The microhardness measurements were made in two different directions and measurement locations, as shown in the measuring diagram (Fig. 3).

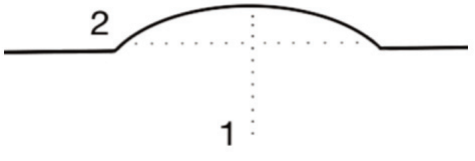

Fig. 3. Hardness measuring scheme: 1 – vertical; 2 – horizontal over the cladding.

3. RESULTS OF LASER EXPERIMENTS

The following chapter outlines the laser cladding experiment results. The influence of the cladding positions is determined and defined, the influence of α is investigated, and the cladding and substrate hardness are identified and further investigated.

3.1. Influence of the cladding nozzle tilting angle

The research determines the influence of α on the cladding characteristics and shape of the cross-section (Fig. 4). It was concluded that a decrease in α values (lower than $\alpha = 90°$) decreases the melting efficiency (E_{pm}) due to a decrease in laser intensity (I_{LP}, W/mm^2) (2), where P – power (W); S – square (mm^2); D – lasers spot diameter (mm) and powder feed intensity (I_{PF}, %) (3).

$$I_{LP} = \frac{P}{S} = \frac{4P \times sin\alpha}{\pi D^2}, \tag{2}$$

$$I_{PF} = \left(0.072 \times \left(\frac{\alpha\pi}{180°}\right) + 0.701\right) \times 100\,. \tag{3}$$

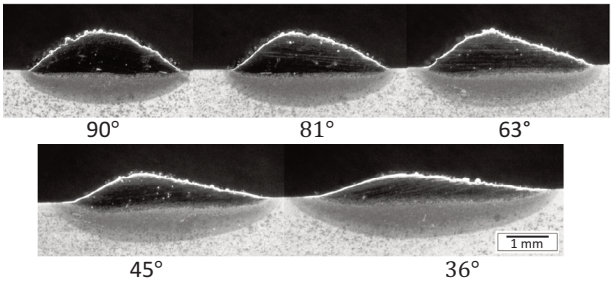

Fig. 4. The influence of on the shape of the cladding cross-section.

It was determined that when I_{LP} was decreased 42% and I_{PF} was decreased 8.5%, the value of A_c decreased 37% at α = 90° compared with A_c results at α = 90°. The percentage values do not reflect the quantitative dependencies of the characteristics and parameters. Therefore, a mathematical expression G (4) has been introduced in the research. G includes all technological parameters, even the nozzle angle and powder feed intensity. The new parameter G describes all experimental parameters that were controlled in a logical manner and the ratio of actual powder feed intensity at the current angle α and powder feed intensity at an angle α = 90°, calculated by Eq. (3). In Chapter 3.2, the parameter G has been used for predicting the result.

3.2. Mathematical expressions used for predicting the laser cladding characteristics

Analysing the results of the laser cladding experiment, it was concluded that it is possible to introduce a new parameter G (4), to describe the laser cladding results. Moreover, Eq. (4) can be simplified and written without the I_{PF} influence. In this way we introduce a simple expression (5) where very little precision is sacrificed.

The mathematical expression (5) was used to predict laser cladding results. Equation (6) was introduced to calculate A_c. Results of those calculations are shown in Fig. 5. In the paper, further expressions to predict H (7) and D_c (8) have been developed.

The variance (9) of the expression (6) has been developed in this work, where each coefficient of the parameter G is expressed by the linear equation, which is described by the proportion of the cladding material density (ρ) and the efficiency of the cladding (E_{pm}, at α = 90°) – E_{pm}/ρ.

It was determined that it is possible to write a linear expression (10) for H calculation from the A_c value.

$$G = \frac{4P \times sin\alpha}{\pi D^2} \times \frac{F_{pm}}{v} \times \frac{\left(0.072 \times \left(\frac{\alpha\pi}{180°}\right)+0.701\right)}{0.814} \left[\frac{Wg}{mm^3}\right], \quad (4)$$

$$G = \frac{4P \times sin\alpha}{\pi D^2} \times \frac{F_{pm}}{v} \left[\frac{Wg}{mm^3}\right], \quad (5)$$

$$A_c = -0.02G^2 + 0.65G + 0.33, \quad (6)$$

$$H = -0.008G^2 + 0.25G + 0.2, \quad (7)$$

$$D_c = 0.7G^2 - 9.77G + 43.64, \quad (8)$$

$$A_c = \frac{\left(-1.7 \times \frac{E_{pm}}{\rho} + 10\right)G^2 + \left(77.83 \times \frac{E_{pm}}{\rho} + 1.11 \times 10^{-12}\right)G + \left(86.5 \times \frac{E_{pm}}{\rho} + 5\right)}{10000}, \quad (9)$$

$$H = 0.38A_c + 0.06. \quad (10)$$

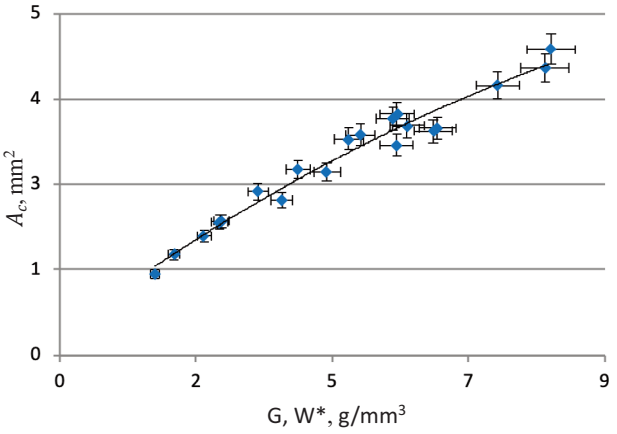

Fig. 5. Parameter G with high precision (96.7%) describes the A_c results, shown with 5% error.

3.3. Influence of the cladding position

The influence of the positions F, VU, OH and VD on the laser cladding characteristics H, A_c and D_c was experimentally determined. The defined coefficients (K_{pos}), summarized in Table 4, are applicable for the nozzle angle α = 36°, the amount of powder transport gas and protective gas supply (3 l/min and 15 l/min, respectively).

3.4. Laser cladding and base material hardness

Analysing the vertical hardness measurements, it was found that the hardness of the cladding layer is slightly influenced by the cladding position (F, OH). These results are shown in Fig. 6, where the negative distances refer to the cladding.

The horizontal measurements of the cladding hardness (Fig. 7) were taken as shown in Fig. 2, scheme 2, about

Table 4. Characteristic coefficients in different nozzle positions at α = 36°

Characteristic	Position No.	Position	Coefficient, K_{pos}
H	1	F	1.0
	2	VU	1.1
	3	OH	0.9
	4	VD	0.9
A_c	1	F	1.0
	2	VU	1.2
	3	OH	0.8
	4	VD	1.1
D_c	1	F	1.0
	2	VU	1.1
	3	OH	1.2
	4	VD	1.1

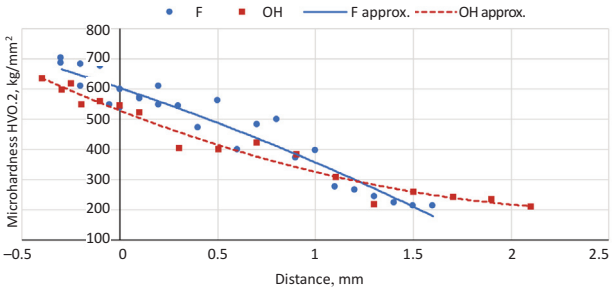

Fig. 6. Vertical microhardness measurements at α = 36°.

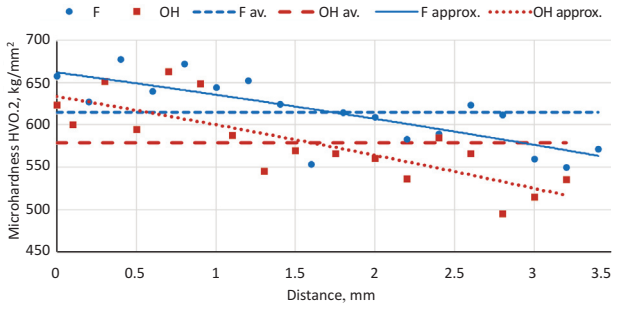

Fig. 7. Horizontal microhardness measurements at α = 36°.

0.1 mm from the top of the base material. In this way, it was possible to identify the changes in the hardness value for an individual cladding profile.

The temperature distribution of the melt pool ("*E-MAqS*" system picture, Fig. 8) and the cladding profile at α = 90° and α = 36° were compared, as well as at α = 36° with the OH position.

It should be noted that in Figs 6 and 7, the reciprocal position is observed, as well as the position of the cladding nozzle at α = 36°, where the left point of the cladding profile (at 0 mm) is the closest to the cladding nozzle.

The combination of these cladding parameters and conditions results in the temperature distribution around

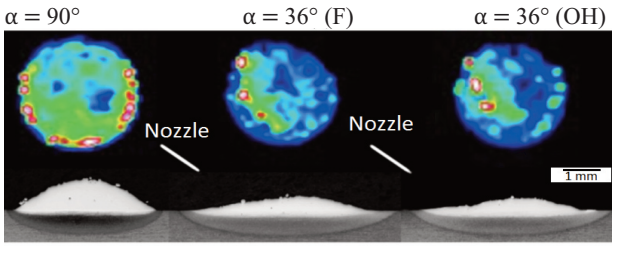

Fig. 8. Temperature distribution of the melt pool ("*E-MAqS*" visualization) and the cladding profile at α = 36° and α = 90°.

the melt pool and the geometry of the melt pool, which have been quantitatively analysed in this work using the *E-MAqS* system. During the cladding process, the number of pixels (T_A) above the set target temperature (1500 °C) was recorded, thus providing numerical information on the cladding conditions.

The obtained data has been summarized by measuring the average T_A value in the cladding process and shows the effect of T_A on the average horizontal HV values (Fig. 9a). The results in Fig. 9b also show how D_c is correlated with the HV values.

4. EXAMINATION OF MATHEMATICAL EXPRESSIONS RELATED TO THE LASER CLADDING AND EXPERIMENT RESULTS

The purpose of this chapter is to compare the calculations of mathematical expressions developed from our results with other experiments that are not related to the development of the expressions: experiment analysing the influence of the cladding position (F, VU, OH and VD) and other authors experiments that were found in the literature.

The accuracy of the A_c, H and D_c expressions (6), (7) and (8) has been tested in this work using the square of the correlation coefficient (R^2) calculated with expression (11) [10] (expression example with A_c), where A_c is the value delivered in the experiment, but A_{cMod} is the calculated value. R^2 indicates how the percentage of cases introduced by the expression and factor G, explain the results of the experiment [15,16, 17].

The results gained from the experiments conducted with different cladding positions and data from the literature [7,18,19,20,21] were used to test the laser cladding expressions developed during research. In the mentioned sources, only the H and D_c experiment results were found; other authors' experiment results were therefore used to examine the A_c expression, which were not associated with the development of the mathematical expressions.

It has been determined that the expression (7) for calculating H estimates 84% of the results and the expression (8) for calculating D_c estimates 38% of the individual results, although 95% of these individual results were approximate. Expression (6), used for calculating A_c, estimates 87% of the results. As an example, A_c results have been summarized in Fig. 10, where the red curve is A_c calculated values, but the individual experiment results are marked with blue points. Results are shown with a 5% error bar and the blue curve is the quadratic approximation of the experimental results.

$$R^2 = \left(\frac{\sum A_c \times A_{cMod} - \frac{\sum A_c \times \sum A_{cMod}}{n}}{\sqrt{\sum A_c^2 - \frac{(\sum A_c)^2}{n}} \times \sqrt{\sum A_{cMod}^2 - \frac{(\sum A_{cMod})^2}{n}}} \right)^2. \quad (11)$$

5. DISCUSSION OF RESULTS

Laser cladding experiments with different nozzle positions (OH, VU and VD) were made possible using a nozzle tilt angle $\alpha = 36°$. The nozzle tilt angle varied due to safety reasons, to prevent damaging experimental equipment and optics. Cladding at position F with $\alpha = 36°$ and other angles made it possible to identify the influence of F on the characteristics.

The cladding characteristics H, A_c and D_c mainly depend on the amount of material supplied on the cladding area, cladding speed and laser power.

It has been experimentally determined that the different nozzle angles (α) have a significant effect on H, A_c and D_c values. It was found that changing α value affects the intensity of the laser power (2) and the powder flow in the cladding zone (3), which ultimately affects the cladding result (Fig. 4).

It is known that material supply (3) is affected by the powder feed and the cladding speed, which is the ratio of the powder feed to the cladding speed (F_{pm}/v). Also, the laser power at the cladding area (2) can be described by the laser power divided by the laser spot area.

Therefore, the authors logically described both expressions I_{LP} (2) and I_{PF} (3) with one main parameter G (4). Equation (4) is simplified to expression (5) – written without the I_{PF} influence (3). For this reason, it is possible that accuracy suffers somewhat. Also, it is not always possible to measure powder flow efficiency, so prediction is made easier using expression (5).

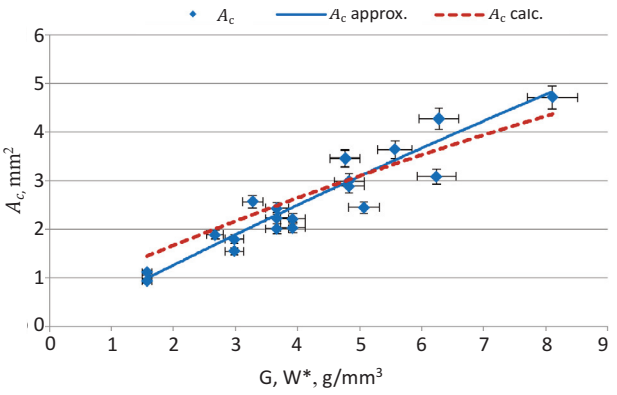

Fig. 10. Effect of parameter G on the surface of the cladding square A_c.

Through the analytical process, it was found that the parameter G (5) correlates with the cladding characteristics H, A_c, and D_c. Therefore, it has been concluded in this work that G (5) is suitable for calculating cladding characteristics. In this process it was decisively shown that G in expression (6) describes 96.7% of the A_c results. Also, expression (7) describes 95.3% of H results, and 81% of D_c results are described with expression (8). These values indicate how well G correlates with cladding results.

The authors introduce Eq. (9) to calculate A_c, where the powder density ρ and cladding efficiency E_{pm} values are used. These may vary when different powder ma-

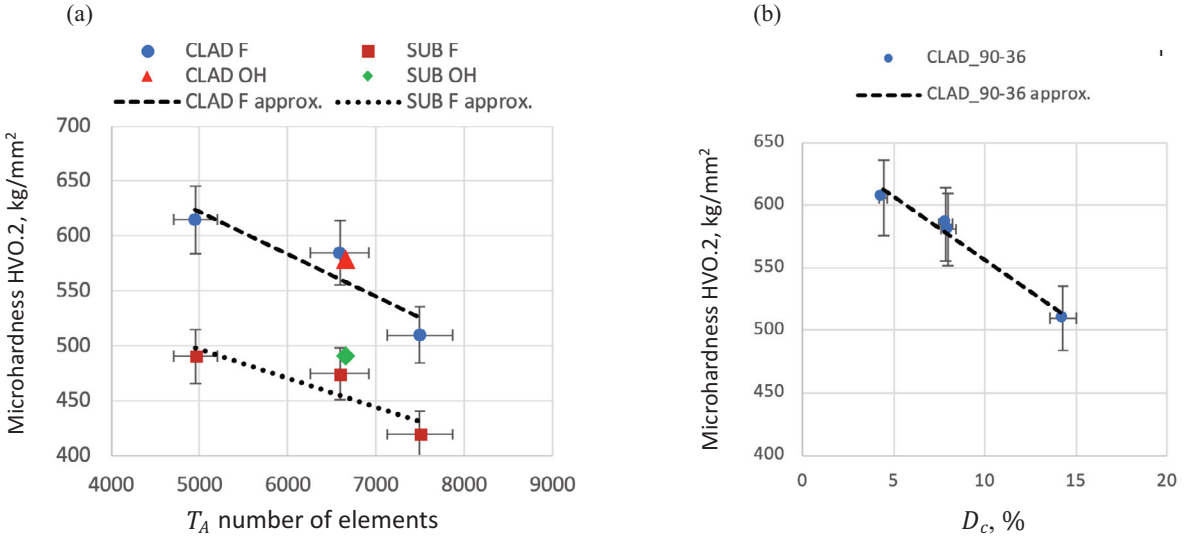

Fig. 9. Dependence of the HV value on T_A at $\alpha = 36°$ and dependence of the HV value on D_c.

terials and cladding nozzles are used. Therefore, mathematical expression (9) has a wider usage than (5), but most challenging is to evaluate the cladding efficiency E_{pm}.

It was determined that A_c and H are correlated, and H can be calculated with the expression (10). Here, A_c describes 92.8% of H results. Expression (10) can be used for quick assumption of results if the A_c value is known, or vice versa, to calculate A_c. The transformation of an elementary expression (10) can be used if H is known.

It was found that the cladding position (F, VU, OH or VD) significantly affects the cladding characteristics; this effect is expressed in the coefficients summarized in Table 4. The introduced coefficients indicate the difference between results that are achieved at the current cladding position and the cladding results in the flat position (F). The coefficients provide an opportunity to predict the cladding results in different cladding positions (VU, OH or VD), by multiplying the Table 4 coefficient K_{pos} with any of the H, A_c, and D_c results at the nozzle position F.

Experiments with universal coaxial nozzle (COAX12) showed that the most suitable nozzle position was F with the nozzle angle $\alpha = 90°$, because in the experimental work it was found that the efficiency E_{pm} at the perpendicular position of the nozzle ($\alpha = 90°$) was achieved with minimal material loss. In addition, the cladding obtained at $\alpha = 90°$ is symmetrical (Fig. 4). However, the powder flow is affected by the gravity in all cladding positions, only in cladding position F this effect is not negative (gravity acts in the direction of the powder flow).

The cladding hardness is slightly influenced by the cladding position F, OH (Fig. 6), where the HV values for OH positions are lower. But for both positions, HV values drop equally when the distance from cladding increases. There is no precise surface measurements of the base material. At a 0 mm distance, it is an approximation but from Fig. 6 we can conclude that the base material hardness is affected up to a depth of approximately 1.5 mm due to dilution and the heat-affected zone.

Figure 7 shows that hardness values are higher in the beginning of the cladding profile when the nozzle angle $\alpha = 36°$ but the values decrease steadily when the distance from the left point of the profile increases. In contrast, looking at the hardness values at the nozzle position $\alpha = 90°$, it was concluded that they are close to the mean values (HV 591 kg/mm^2) throughout the length of the profile. From this we can conclude that the stability of the horizontal HV value depends on α.

From Fig. 8 it can be seen that the melt pool temperature distribution also depends on α in the same way as the HV result in Fig. 7. It has been found that the melt pool temperature distribution is mainly influenced by the powder flow intensity and the shape of the laser point, and both depend on α. When $\alpha < 90°$, the highest powder flow intensity is in the middle, but on the farthest cladding zone, the powder flow intensity is significantly higher compared to the closest zone. For a round laser point, the action time of the laser beam is shorter on the profile edges compared to the middle part of the profile, due to the differences in distances between round point segments. If at $\alpha < 90°$ the laser point is oval, the action time difference is greater. This shorter action time results in more rapid cooling of the cladding and the base material, which contributes to the formation of higher HV values at the edges of the cladding profile (Fig. 7).

From Fig. 9a it can be seen that samples with a higher T_A have lower HV values, and this is true for both the cladded layer and the base material HV values. Also, Fig. 9a shows independent OH cladding T_A and HV values for the cladding (red point) and the base material (green point). Both OH position values fit into a 5% error bar. Knowing that T_A indicates a melt pool size, if T_A increases, D_c also increases. Therefore, Fig. 9b shows that D_c values correlate with HV values in the same way as T_A.

Analysis of the cross-sectional hardness demonstrated that laser cladding with Stellite® 6 powder (Table 2) provides 2.8 times higher hardness compared to the base material S355J2.

6. CONCLUSIONS

Laser cladding technology with powder can be implemented in the F, VU, OH and VD positions. Cladding in the OH position is made possible by using a COAX12 nozzle at an angle $\alpha = 36°$. The characteristic coefficients A_c, H and D_c in the F, VU, OH and VD positions were introduced in Table 4. Coefficient K_{pos} shows the difference in results at any cladding positions by multiplying it with F position.

It can be concluded from the work that the cladding characteristics A_c, H and D_c depend on the amount of material, cladding speed and laser power used at the current cladding area and the nozzle angle α. Therefore, parameter G (5) is introduced to describe all the laser cladding parameters used. The parameter G correlates with A_c, H and D_c. This provided the basis to develop the mathematical expressions from G to determine the laser cladding characteristics A_c (6), H (7) and D_c (8). The validity of the developed mathematical expressions (6), (7) and (8) was verified using the square of the correlation coefficient R^2 (11). It revealed that the mathematical expression (6) for A_c calculation explains 87% of the H results, expression (7) explains 84% of H results and (8) explains 38% of D_c results. It was concluded that the developed mathematical expressions show a high degree of precision.

After evaluating the obtained HV results, it has been concluded that the mechanical properties of the cladding depend on the shape of the laser point, the intensity of the powder flow, the cladding position and the nozzle angle. As it affects the temperature distribution of the cladding melt pool (Fig. 8), this describes the obtainable HV value of the cladding profile (Figs 7 and. 9). It has been proved that D_c is directly influenced by the T_A value, which affects HV. This indicates that the information provided by T_A is applicable to the evaluation of the cladding conditions and the determination of the characteristics, but more in-depth studies of this will be required in the future.

It was concluded that using coaxial nozzle for laser cladding enabled to achieve higher cladding efficiency values with the F cladding position and perpendicular position of the nozzle ($\alpha = 90°$). Also, $\alpha = 90°$ results in the smoothest HV values. In order to achieve the best laser cladding results, F_{pm}/v = 28 g/m – 65 g/m.

The knowledge from this research is adaptable and applicable to development of cladding external surfaces.

ACKNOWLEDGEMENTS

The publication was supported by Riga Technical University Development Fund. The publication costs of this article were partially covered by the Estonian Academy of Sciences.

REFERENCES

1. Bach, Fr.-W., Laarmann, A., and Wenz, T. (eds). *Modern Surface Technology*. Wiley-VCH Verlag GmbH & Co. KGaA, Weinheim, 2006.
2. Fischer, A. and Bobzin, K. (eds). *Friction, Wear and Wear Protection*. Wiley-VCH Verlag GmbH & Co. KGaA, Weinheim, 2009.
3. Bartels, F., Jonnalagadda, A., Wiener, M., and Stiles, E. Laser cladding of tubes. US Patent 9,126,286B2, 8 September 2015. https://patentimages.storage.googleapis.com/b7/eb/dc/c6c78275815a61/US9126286.pdf
4. Inner diameter coating system COAXid. https://www.iws.fraunhofer.de/en/business_fields/surface_treatment/laser_cladding/system_technology/COAXid.html (accessed 2020-04-22).
5. Bady, T., Bohling, M., Lensch, G., Fischer, A., Feikus, F.-J., and Sach, A. Process and device for laser treatments of inside surfaces. US Patent 6,303,897, 16 October 2001.
6. Cheikh El, H., Courant, B., Branchu, S., Hascoët, J.-Y., and Guillén, R. Analysis and prediction of single laser tracks geometrical characteristics in coaxial laser cladding process. *Opt. Lasers Eng.*, 2012, **50**(3), 413–422.
7. Guo, S., Chen, Z., Cai, D., Zhang, Q., Kovalenko, V., and Yao, J. Prediction of simulating and experiments for co-based alloy laser cladding by HPDL. *Phys. Procedia*, 2013, **50**, 375–382.
8. Sun, Y. and Hao, M. Statistical analysis and optimization of process parameters in Ti6Al4V laser cladding using Nd:YAG laser. *Opt. Lasers Eng.*, 2012, **50**(7), 985–995.
9. Tabernero, I., Lamikiz, A., Ukar, E., López de Lacalle, L. N., Angulo, C., and Urbikain, G. Numerical simulation and experimental validation of powder flux distribution in coaxial laser cladding. *J. Mater. Process. Technol.*, 2010, **210**(15), 2125–2134.
10. Zhang, K., Liu, W., and Shang, X. Research on the processing experiments of laser metal deposition shaping. *Opt. Laser Technol.*, 2007, **39**(3), 549–557.
11. Hofman, J. T., de Lange, D. F, Pathiraj, B., and Meijer, J. FEM modeling and experimental verification for dilution control in laser cladding. *J. Mater. Process. Technol.*, 2011, **211**(2), 187–196.
12. Modular powder nozzle system COAXn. https://www.iws.fraunhofer.de/en/business_fields/surface_treatment/laser_cladding/system_technology/COAXn.html (accessed 2020-04-27).
13. EN 10025-2 S355J2 high strength structural steel plate. http://www.steelspecs.com/EN10025-2/EN10025-2S355J2STEELPLATE.html (accessed 2020-06-02).
14. Kennametal Stellite alloys. https://www.kennametal.com/content/dam/kennametal/kennametal/common/Resources/Catalogs-Literature/Stellite/B-18-05723_KMT_Stellite_Alloys_Brochure_Direct_update_LR.pdf (accessed 2014-07-07).
15. Antony, J. *Design of Experiments for Engineers and Scientists*. Butterworth Heinemann, Burlington, 2003.
16. Montgomery, D. C. *Design and Analysis of Experiments, 5th Ed*. John Wiley & Sons, Weinheim, 2001.
17. Mason, R. L., Gunst, R. F., and Hess, J. L. *Statistical Design and Analysis of Experiments*: *With Applications to Engineering and Science, 2nd Ed*. John Wiley & Sons, New Jersey, 2003.
18. Lin, C.-M. Parameter optimization of laser cladding process and resulting microstructure for the repair of tenon on steam turbine blade. *Vacuum*, 2015, **115**, 117–123.
19. Saqib, S., Urbanic, R. J., and Aggarwal, K. A. Analysis of laser cladding bead morphology for developing additive manufacturing travel paths. *Procedia CIRP*, 2014, **17**, 824–829.
20. Sohrabpoor, H. Analysis of laser powder deposition parameters: ANFIS modeling and ICA optimization. *Optik*, 2016, **127**, 4031–4038.
21. Zhang, K., Liu, W., and Shang, X. Research on the processing experiments of laser metal deposition shaping. *Opt. Laser Technol.*, 2007, **39**(3), 549–557.